

Blood cell counting based on U-Net++ and YOLOv5*

BAI Hua¹, WANG Xuechun¹, GUAN Yingjian², GAO Qiang^{1**,} and HAN Zhibo^{3,4**}

1. Tianjin Key Laboratory of Optoelectronic Detection Technology and Systems, School of Electronic and Information Engineering, Tiangong University, Tianjin 300387, China

2. Shenzhen Weian Co-create Biotechnology Co., Ltd., Shenzhen 518000, China

3. Tianjin Key Laboratory of Engineering Technologies for Cell Pharmaceutical, Tianjin 300457, China

4. National Engineering Research Center of Cell Products / AmCellGene Co., Ltd., Tianjin 300457, China

(Received 8 October 2022; Revised 18 January 2023)

©Tianjin University of Technology 2023

Clinical information about a variety of disorders is available through blood cell counting, which is usually done by manual methods. However, manual methods are complex, time-consuming and susceptible to the subjective experience of inspectors. Although many efforts have been made to develop automated blood cell counting algorithms, the complexity of blood cell distribution and the highly overlapping nature of some red blood cells (RBCs) remain significant challenges that limit the improvement of analytical accuracy. Here, we proposed an end-to-end method for blood cell counting based on deep learning. Firstly, U-Net++ was used to segment the whole blood cell image into several regions of interest (ROI), and each ROI contains only one single cell or multiple overlapping cells. Subsequently, YOLOv5 was used to detect blood cells in each ROI. Specifically, we proposed several strategies, including fine classification of RBCs, adaptive adjustment for non-maximal suppression (NMS) threshold and blood cell morphology constraints to improve the accuracy of detection. Finally, the detection outcomes for each ROI were combined and superimposed. The results show that our method can effectively address the issue of high overlap and precisely segment and detect blood cells, with a 98.18% accuracy rate for blood cell counting.

Document code: A **Article ID:** 1673-1905(2023)06-0370-7

DOI <https://doi.org/10.1007/s11801-023-2165-3>

In biomedicine, a complete blood count (CBC) is used to determine the quantity of blood cells in order to evaluate the patient's physical health. Red blood cells (RBCs) rank first in number in blood cells and serve as the connector and transporter of O₂ and CO₂. So, changes in the number and morphology of RBCs can provide information for the diagnosis of diseases, such as anemia, leukemia, and other blood disorders^[1]. In addition, the main role of the immune system against pathogens is white blood cells (WBCs). A deviation in the number of WBCs indicates the potential diseases of infections, serious tissue damage, as well as leukemia, malignant tumors, etc^[2]. Traditionally, blood cell counting is done manually using hematology analyzers which use grids for counting^[3] and use averages to suppress the influences of instruments and blood sample concentrations. However, the manual methods are cumbersome and time-consuming, especially in the situation of large numbers of blood samples. Also, subjective factors often lead to biased calculation results. Therefore, automated blood cell counting has become one of the research hotspots in the field of medical image analysis.

In recent years, many automated blood cell counting

algorithms have been proposed. For example, MAZALAN et al^[4] proposed a method to calculate the total number of erythrocytes in peripheral blood smear images using the circular Hough transform (CHT). YAZAN et al^[5] presented an automatic segmentation counting method for erythrocytes and leukocytes based on an iterative structural circle detection algorithm. LI et al^[6] proposed a combined spatial and spectral erythrocyte recognition algorithm that combines an active contour model and an automatic two-dimensional K-means and spectral angle mapping algorithm. APARNA et al^[7] proposed a simulation model for anemia detection based on an RBC counting algorithm, using two methods, CHT and connected component labeling, to count RBCs respectively. Although these algorithms can solve most of the blood cell counting issues, they still face the following challenges. The cell distribution is complex. There are not only areas with single blood cell (as shown by red dashed line in Fig.1), but also areas where multiple blood cells are adherent. Moreover, the adhesion of blood cells varies greatly between different areas (as shown by the yellow dashed line in Fig.1). In the area of multicellular adhesion, some of the RBCs overlap to an extremely

* This work has been supported by the National Natural Science Foundation of China (No.61201106), and the Tianjin Special Program of Science and Technology (No.19JCTPJC47900).

** E-mails: gaoqiang@tiangong.edu.cn; zhibohan@163.com

high degree (as shown by the green dashed line in Fig.1), posing a great challenge to the accurate detection and counting of RBCs.

Deep learning^[8] has recently developed quickly and has been applied gradually to biomedical field. The convolutional neural network (CNN)^[9] is one of the representative algorithms of deep learning with the representation learning capability. It can learn the key features of targets automatically by training and perform translational invariant classification of the targets. Therefore, CNN is potential to provide a more powerful tool to solve the above problems.

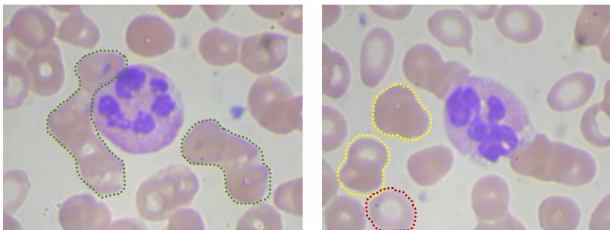


Fig.1 Typical blood cell micrographs (The areas marked with red, yellow and green dashed lines represent single cell, adherent cells and highly overlapping cells respectively)

In this respect, CHOWDHURY *et al*^[10] developed a low-cost automated system based on CNN to recognize and count RBCs, different types of leukocytes, and identify malaria infection from digital blood smear images. CHOURASIYA *et al*^[11] designed an efficient and cost-effective computer vision system for automatic RBC counting using image-based analysis. DHIEB *et al*^[12] designed a new framework using CNN, migration learning, and mask R-CNN to automatically count and classify different blood cells in a given microscopic blood smear image. WANG *et al*^[13] used faster R-CNN with a ResNet-101 backbone to analyze blood cell images captured with an optical microscope and camera. These methods show the great potential of deep learning in blood cell counting, but highly overlapping cell count is still a difficult issue.

Many attempts have been made to solve this problem caused by highly overlapping cells. For example, ZHANG *et al*^[14] used YOLOv3 to detect discrete RBCs, white blood cells and aggregated RBCs in microscopic images and subsequently counted the aggregated RBCs using the image density estimation method. INCHUR *et al*^[15] proposed a digital image processing technique to accurately count all the blood cells in a given slide with maximum accuracy. A method, such as morphological operator, texture-based classification method and CHT, was used to count the RBC. JIANG *et al*^[16] used Hessian matrices to obtain cell density maps combined with multiple random forests to predict cell density maps and to count overlapping cells. TESSEMA *et al*^[17] proposed a method for automatic classification and quantitative analysis of blood cells using the YOLOv2 model. ZHOU

et al^[18] designed a pipeline of erythroid-counter consisting of a detection and extraction module (DEM) and a classification counting module (CCM) for fully automated detection and classification of RBCs. NARDO-MARINO *et al*^[19] proposed a new automated workflow for counting RBCs with depressions. They used a Zeiss Intellesis deep learning model to recognize and segment cells and pits in DIC images, and then used a small ImageJ macro language script to analyze the segmented images. These methods have made great progress in blood cell counting, but further research is still needed due to the diversity and complexity of the overlapping cells.

In this paper, we proposed a new method for blood cell counting based on U-Net++^[20] and YOLOv5^[21], as shown in Fig.2. Its key steps are as follows. Firstly, U-Net++ is used to segment the whole blood cell image into several regions of interest (ROI), and each ROI contains only one single cell or multiple adherent cells. It can not only remove the noises, but also simplify the complex cell distribution. Then, YOLOv5 is used to detect RBCs and WBCs in each ROI. In particular, we proposed an adaptive non-maximal suppression (NMS) threshold adjustment algorithm, which can adjust the NMS threshold adaptively according to the overlapping degree of RBCs, to improve the detection of highly overlapping RBCs and avoid the duplicate detection boxes. Moreover, fine classification of RBCs and erythrocyte morphology constraints were proposed to further improve the accuracy of detection. Finally, the detection outcomes of all ROIs are combined and superimposed.

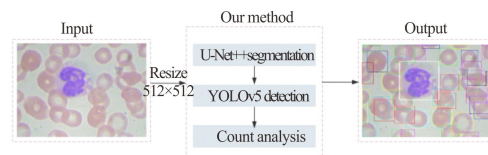


Fig.2 Schematic diagram of our blood cell counting method

The dataset we chose is the blood cell dataset BCCD, published on Kaggle. The dataset consists of 364 640×480 images. In our study, all the images were uniformly resized to 512×512 for subsequent ease of operation.

The U-Net++ network is used to segment RBCs and WBCs from the background in order to simplify the whole blood cell image into several ROIs, each of which contains one single cell or multiple adherent cells.

The U-Net++ we used for blood cell segmentation is shown in Fig.3. It uses the ResNet-50 as the backbone, and embeds U-Nets^[22] of 4 depths, skip connections and deep supervision. The skip connections allow the introduction of high-resolution information from the blood cell microscopy image into the results obtained by up-sampling, ensuring segmentation accuracy. The deep supervision allows the model to perform pruning operations, making the model more flexible and general. A

1×1 convolution with a 3-kernel (corresponding to RBCs, WBCs and background, respectively) and a Sigmoid activation function is attached to the output nodes $x^{(0,1)}$, $x^{(0,2)}$, $x^{(0,3)}$, and $x^{(0,4)}$ to get a final output.

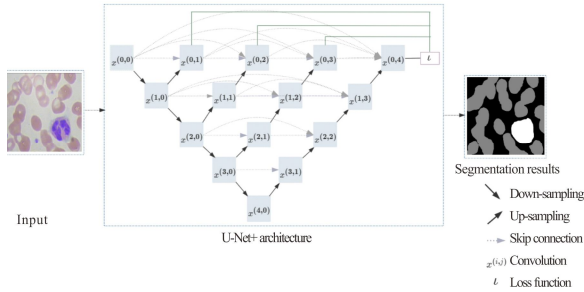


Fig.3 Structure of U-Net++ network for blood cell segmentation^[20]

The YOLOv5 network is used for blood cell detection. As shown in Fig.4, the network consists of three parts. Backbone is used for feature extraction, mainly including the CSP module and the SPP module to enhance the model's ability to capture features. Neck is the structure of the feature pyramid network (FPN)^[23] combined with PAN. The semantic information extracted from the deep network is fused with the information from the shallow network to obtain richer feature information and enhance the detection capability for targets at different scales. Head is used to predict the detection boxes.

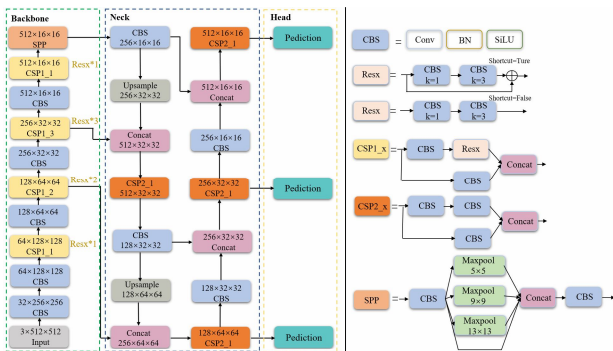


Fig.4 Network structure diagram of YOLOv5^[21]

For the cell segmentation by U-Net++, 120 blood cell micrographs were used for training. These images were further expanded to 960 images through rotation and mirror operation. The training was performed on a Nvidia Tesla V100 GPU platform, the initial learning rate was set to 0.000 1, and the gradient descent was performed using the Adam algorithm.

The segmentation effect is shown in Fig.5, where the white, gray and black areas represent WBCs, RBCs and background, respectively. It can be seen that the interference of impurities and platelets can be accurately excluded (as shown in the white boxes). What's more, the blood cells can keep their original shape well, and no false deletion of blood cells is found during the denoising process. The results demonstrate the excellent performance of U-Net++ in the blood cell segmentation. Further, each segmented area is extracted as an ROI, and thus the

complex cell distribution can be decomposed into several ROI subgraphs, each of which contains one single cell or multiple adherent cells.

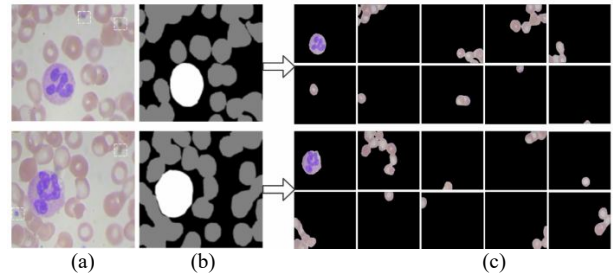


Fig.5 Blood cell segmentation: (a) Original micrographs; (b) Segmentation results by U-Net++; (c) ROI extraction

After the extraction of the ROIs, we used the YOLOv5 network to detect RBCs and WBCs from each ROI, and then combined the detection outcomes of all ROIs to generate a final output. The training of YOLOv5 was also performed on the Nvidia Tesla V100 GPU platform, the initial learning rate was set to 0.01, the gradient descent was performed using the Adam algorithm, and the training set and validation set were from the ROI images. Before training, we pre-trained the YOLOv5 on VOC2007 to obtain a pre-trained model, which can significantly improve the speed and accuracy of the training.

The typical detection result by YOLOv5 is shown in Fig.6. It can be seen that single RBCs, adherent or slightly overlapping RBCs and the WBC can be accurately detected (RBCs are indicated by green boxes and the WBC by white box). However, the following problems still exist, including false detection of multiple high overlapping RBCs as one cell (as shown by the red dotted curves), and missed detection of some morphologically irregular RBCs and high overlapping RBCs (as shown by the yellow dotted curves). In order to improve the performance of the model, we proposed three strategies including fine classification of RBCs, adaptive NMS threshold adjustment, and morphological constraints.

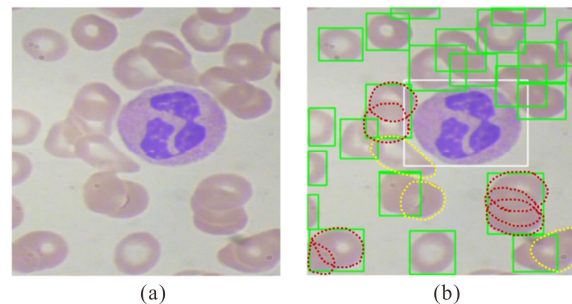


Fig.6 Detection of blood cells by YOLOv5: (a) Original micrograph; (b) Detection result

Since a single classification of RBCs is difficult to cover the complex cases, which are due to the individual

differences of RBCs in shape and the cell distribution, we proposed a fine classification of RBCs. In terms of shape, RBCs show two typical shapes, round and oval. In terms of distribution, most highly overlapping RBCs are partially hidden by other RBCs, thus showing obvious morphological differences from single RBCs. Therefore, we divided the category of RBCs into three separate categories, round RBCs, elliptical RBCs, and hidden RBCs.

The YOLOv5 network with fine classification of RBCs was retrained, and the comparison of the detection results with and without this strategy is shown in Fig.7. It can be seen that the fine classification significantly improves the detection of RBCs. Specifically, some irregularly shaped RBCs are successfully detected (as shown by the red boxes in Fig.7(b)), confirming the effectiveness of this strategy. However, the detection of highly overlapping RBCs still needs further improvement.

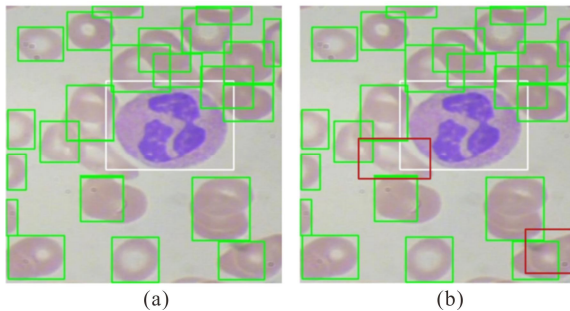


Fig.7 Comparison of the detection results (a) without and (b) with fine classification of RBCs

For each target, the NMS algorithm can remove duplicate detection boxes by selecting the box with local maximum confidence score and removing other boxes with large overlap with the selected box. It sets a threshold of intersection ratio, the higher the threshold, the larger the overlap between detection boxes can be allowed, and vice versa.

Obviously, due to the complexity of the cell distribution, each ROI's cell distribution may differ from another, making it difficult to analyze all ROIs using a fixed threshold. Specifically, for a single RBC, the threshold is expected to be lower to remove duplicate detection boxes. On the contrary, for the highly overlapping RBCs, the threshold is expected to be higher to avoid missed detection of the cells. For example, Fig.8 shows the detection results of two ROIs at different NMS thresholds, respectively. When the NMS threshold is 0.1, there are missed detections in the both ROIs. As the NMS threshold increases, the missed detections in both ROIs decrease gradually. When the NMS threshold reaches 0.25, the RBCs in ROI (a) are completely detected, but some RBCs in ROI (b) remain undetected until the NMS increases to 0.28. When the NMS threshold further increases to 0.60, redundant detection boxes appear in both ROIs. As can be observed, different ROIs have different

best NMS thresholds to match.

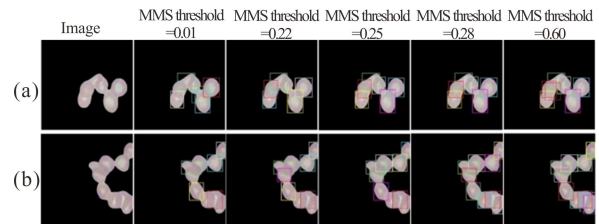


Fig.8 Detection of highly overlapping RBCs at different NMS thresholds ((a) and (b) are two representative ROIs)

Therefore, we proposed an adaptive NMS threshold adjustment algorithm to determine the best NMS threshold for each ROI according to the cell distribution. Specifically, the algorithm iterates the NMS threshold between 0.1 and 0.655 in steps of 0.01, and defines the area of RBCs not covered by the detection boxes as the “e” value. For most ROIs containing multiple RBCs, as the NMS threshold increases gradually, “e” shows a step-wise downward trend until it flattens out, and the turning point is selected as the best NMS threshold. On the contrary, for the ROIs containing single RBCs, “e” generally remains constant, and 0.1 is selected as the best NMS threshold.

The comparison of the detection results with and without adaptive NMS threshold adjustment is shown in Fig.9. It can be seen that the strategy of adaptive NMS threshold adjustment makes highly overlapping RBCs detected successfully (as shown by the red boxes in Fig.9(b)), and thus further improves the detection accuracy on the basis of the fine classification of RBCs.

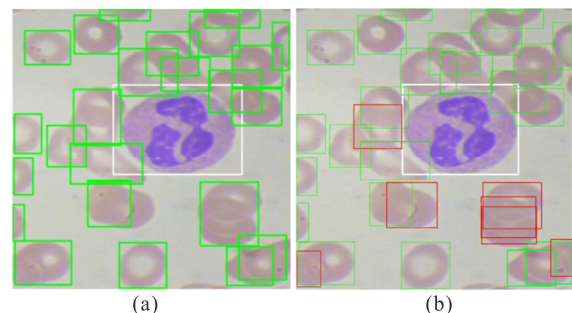


Fig.9 Comparison of the detection results (a) without and (b) with adaptive NMS threshold adjustment

The two strategies mentioned above can solve most problems of the cell detection. However, a few false detection boxes still exist, which recognize multiple overlapping RBCs as a single RBC or cannot accurately mark the position of the cells, as shown in Fig.10(a).

It is found that these false detection boxes have high confidence scores and thus cannot be removed by the NMS algorithm. However, it can be observed that the size of most false detection boxes cannot match the morphological characteristics of RBCs. Therefore, according to the morphological characteristics of RBCs, we

set constraints for the detection boxes in terms of area, length-width ratio and duty ratio to exclude the false detection boxes. The detection results after adding morphological constraints are shown in Fig.10(b). It is obvious that this strategy can remove the false detection boxes effectively, and thus further increase the accuracy of the cell detection.

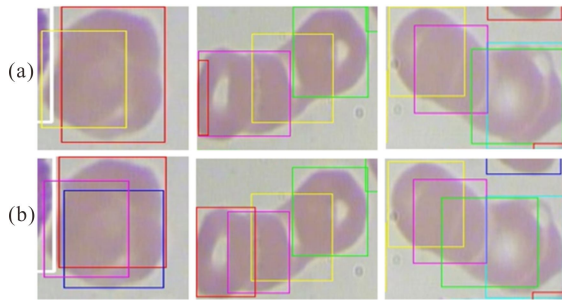


Fig.10 Comparison of the detection results (a) without and (b) with morphological constraints

A typical final detection output by our method is shown in Fig.11. It can be seen that our method can accurately detect each blood cell, whether for WBCs, single RBCs or multiple adherent RBCs, showing a strong adaptability to the complex cell distribution. In particular, our method exhibits an excellent performance in the detection of highly overlapping RBCs, as shown in Fig.11(c) and (d).

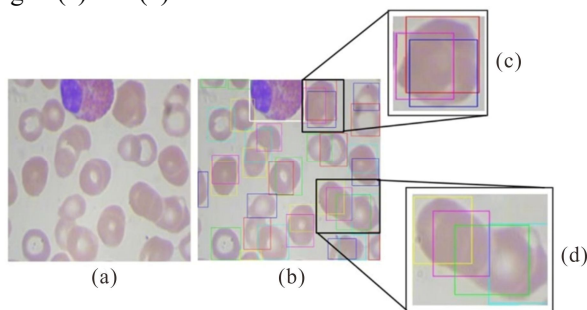


Fig.11 Typical final detection output by our method: (a) Original micrograph; (b) Detection result; (c) and (d) Detection of highly overlapping RBCs

In order to evaluate the effectiveness of our method statistically, we quantitatively analyzed the accuracy of blood cell counting. Here, the definition of the accuracy is shown as

$$Accuracy = \frac{N_{correct}}{\max\{N_{count}, N_{truth}\}} \times 100\%, \quad (1)$$

where $N_{correct}$ is the number of correctly counted blood cells including WBCs and RBCs. N_{count} is the total number of blood cells detected by the method. N_{truth} is the actual total number of blood cells. $\max\{N_{count}, N_{truth}\}$ is the maximum value between N_{count} and N_{truth} . This definition can cover the influences of false detection, missed detection and redundant detection boxes, and thus comprehensively reflect the accuracy of the cell counting.

We randomly picked 100 original micrographs that were not used for training to calculate the accuracy. The micrographs contained 2 913 blood cells, in which 1 970 overlapped blood cells were included. These blood cells were well representative and can be used to assess the accuracy of the method. As a result, the accuracy of blood cell counting reaches 98.18%.

Further, the results of our method are compared with those of the leading methods in the literature, as shown in Tab.1. It can be seen that our method can not only detect highly overlapping cells in terms of function, but also be superior to the current state-of-the-art (SOTA) methods in terms of accuracy. Thus, our method can provide a new powerful tool for blood cell counting.

Blood cell counting is a prerequisite for diagnosis of some disease, but it remains a challenge for many traditional image processing algorithms based on manual rules. In this respect, deep learning can automatically learn the features of the targets through training, and analyze the images based on the learned features rather than artificial rules, so it may provide new ideas to solve this problem.

A challenge of blood cell counting by deep learning is the complexity of cell distribution. As shown in Fig.1, the micrographs contain WBCs, RBCs, platelets and

Tab.1 Comparison of our results with those in the literature

Method	Detection of overlapping blood cells	Actual number of blood cells	Accuracy
Mazalan et al (2013) ^[4]	No	3617	91.87%
Chourasiya et al (2014) ^[11]	Yes	4570	92%
Dhieb et al (2019) ^[12]	Yes	24000	94%
Pengfei et al (2019) ^[14]	Yes	1920	86.49%
Inchur et al (2020) ^[15]	Yes	5700	90%
Tessema et al (2021) ^[17]	Yes	1693	92.96%
Geng et al (2021) ^[13]	No	3206	97%
Proposed method	Yes	2913	98.18%

other impurities. In terms of cell distribution, the micrographs contain single cells, multiple adhesive cells and multiple highly overlapping cells. It is difficult for a target detection network to deal with these complex cases simultaneously. Therefore, we propose an idea of "making the complex distribution simple". That is, a segmentation network is used to segment and extract the WBCs and RBCs to simplify the original micrographs into several ROI subgraphs. Then a target detection network with adaptive NMS threshold adjustment is used to detect the blood cells of each ROI subgraph. Here, the U-Net++ is used for the cell segmentation. It fuses features at several different levels indirectly through operations such as short connections, up and down sampling, and thus has prominent advantages in processing medical images with a small number of samples. The results (Fig.5) show that the U-Net++ exhibits an excellent performance in image denoising and blood cell segmentation. In addition, the YOLOv5 is used for the cell detection. It is a one-stage target detection algorithm that treats target detection as a regression problem and does not require a complex process of candidate boxes generation. Therefore, it is faster than those two-stage algorithms such as faster R-CNN^[24] and fast RCNN^[25]. More importantly, the adaptive NMS threshold adjustment algorithm proposed in this paper can automatically determine the optimal NMS threshold according to the cell distribution of each ROI, and thus greatly improve the accuracy of YOLOv5 for the cell detection (as shown in Fig.9).

Another challenge of blood cell counting by deep learning is the diversity of RBCs' shapes. Especially, the high overlap makes many RBCs partially hidden, which shows different morphological characteristics from single RBCs. It is difficult for the YOLOv5 to recognize the RBCs with obviously different morphological characteristics. Therefore, we propose a strategy of fine classification of RBCs, which greatly enhanced the ability of YOLOv5 to recognize the RBCs (as shown in Fig.7).

In addition, some false detection boxes with high confidence scores are also an important factor affecting the accuracy of the cell detection. Their high confidence scores make them unable to be removed by the NMS algorithm, but make some correct boxes excluded. Thus, we propose a strategy that sets constraints for the detection boxes in terms of area, length-width ratio and duty ratio according to the morphological characteristics of RBCs. The results (Fig.10) show that this strategy is able to exclude the false detection boxes effectively, and thus further improve the accuracy of the cell detection.

The effectiveness of the strategies mentioned above is further confirmed in Fig.11 and Tab.1. The results demonstrate that our method can effectively address the issues of the complex cell distribution and the high overlap of RBCs, with a blood cell counting accuracy of 98.18%, which is superior to the current SOTA methods listed in Tab.1. In addition to the blood cell detection, our method can also provide a valuable reference for detecting other highly overlapping targets.

In this study, we proposed an end-to-end blood cell counting method based on an optimized combination of U-Net++ and YOLOv5. The method consists of three steps. First, the WBCs and RBCs are segmented respectively by the U-Net++, and several ROI subgraphs are generated. Next, the blood cells in each ROI subgraph are detected using an improved YOLOv5, which is optimized by the strategies including fine classification of RBCs, adaptive NMS threshold adjustment and morphological constraints. Finally, the detection outcomes of all ROIs are combined to generate a final output. The results show that our method has an excellent performance in dealing with the complex cell distribution and the high overlap of RBCs, with an accuracy of 98.18% for blood cell counting.

Ethics declarations

Conflicts of interest

The authors declare no conflict of interest.

References

- [1] THEJASHWINI M, PADMA M C. Counting of RBC's and WBC's using image processing technique[J]. International journal on recent and innovation trends in computing and communication, 2015, 3(5): 2948-2953.
- [2] OTHMAN M Z, MOHAMMED T S, ALI A B. Neural network classification of white blood cell using microscopic images[J]. International journal of advanced computer science and applications, 2017, 8(5): 99-104.
- [3] KHAN S, KHAN A, KHATTAK F S, et al. An accurate and cost effective approach to blood cell count[J]. International journal of computer applications, 2012, 50(1): 975-8887.
- [4] MAZALAN S M, MAHMOOD N H, RAZAK M A A. Automated red blood cells counting in peripheral blood smear image using circular Hough transform[C]//2013 1st International Conference on Artificial Intelligence, Modelling and Simulation, December 3-5, 2013, Kota Kinabalu, Malaysia. New York: IEEE, 2013: 320-324.
- [5] AIOMARI Y M, SHEIKH ABDULLAH S N H, ZAHARATUL AZMA R, et al. Automatic detection and quantification of WBCs and RBCs using iterative structured circle detection algorithm[J]. Computational and mathematical methods in medicine, 2014, 2014(8): 979302.
- [6] LI Q, ZHOU M, LIU H, et al. Red blood cell count automation using microscopic hyperspectral imaging technology[J]. Applied spectroscopy, 2015, 69(12): 1372-1380.
- [7] APARNA V, SARATH T V, RAMACHANDRAN K I. Simulation model for anemia detection using RBC counting algorithms and watershed transform[C]//2017 International Conference on Intelligent Computing, Instrumentation and Control Technologies (ICICT), June 15-16, 2017, Madurai, India. New York: IEEE,

- 2017: 284-291.
- [8] LECUN Y, BENGIO Y, HINTON G. Deep learning[J]. *Nature*, 2015, 521(7553): 436-444.
- [9] GU J, WANG Z, KUEN J, et al. Recent advances in convolutional neural networks[J]. *Pattern recognition*, 2018, 77: 354-377.
- [10] CHOWDHURY A B, ROBERSON J, HUKKOO A, et al. Automated complete blood cell count and malaria pathogen detection using convolution neural network[J]. *IEEE robotics and automation letters*, 2020, 5(2): 1047-1054.
- [11] CHOURASIYA S, RANI G U. Automatic red blood cell counting using watershed segmentation[J]. *Hemoglobin*, 2014, 14: 17.
- [12] DHIEB N, GHAZZAI H, BESBES H, et al. An automated blood cells counting and classification framework using mask R-CNN deep learning model[C]//2019 31st International Conference on Microelectronics (ICM), December 15-18, 2019, Cairo, Egypt. New York: IEEE, 2019: 300-303.
- [13] WANG G, ZHAO T, FANG Z, et al. Experimental evaluation of deep learning method in reticulocyte enumeration in peripheral blood[J]. *International journal of laboratory hematology*, 2021, 43(4): 597-601.
- [14] ZHANG D, ZHANG P, WANG L. Cell counting algorithm based on YOLOv3 and image density estimation[C]//2019 IEEE 4th International Conference on Signal and Image Processing (ICSIP), July 19-21, 2019, Wuxi, China. New York: IEEE, 2019: 920-924.
- [15] INCHUR V B, PRAVEEN L S, SHANKPAL P. Implementation of blood cell counting algorithm using digital image processing techniques[C]//2020 International Conference on Recent Trends on Electronics, Information, Communication & Technology (RTEICT), November 12-13, 2020, Bangalore, India. New York: IEEE, 2020: 21-26.
- [16] JIANG N, YU F. A cell counting framework based on random forest and density map[J]. *Applied sciences*, 2020, 10(23): 8346.
- [17] TESSEMA A W, MOHAMMED M A, SIMEGN G L, et al. Quantitative analysis of blood cells from microscopic images using convolutional neural network[J]. *Medical & biological engineering & computing*, 2021, 59(1): 143-152.
- [18] ZHOU Y, WANG Y, WU J, et al. ErythroidCounter: an automatic pipeline for erythroid cell detection, identification and counting based on deep learning[J]. *Multimedia tools and applications*, 2022, 81(18) : 25541-25556.
- [19] NARDO-MARINO A, BRAUNSTEIN T H, PETERSEN J, et al. Automating pitted red blood cell counts using deep neural network analysis: a new method for measuring splenic function in sickle cell anaemia[J]. *Frontiers in physiology*, 2022, 13.
- [20] ZHOU Z, RAHMAN SIDDIQUEE M M, TAJBAKHS N, et al. Unet++: a nested U-net architecture for medical image segmentation[J]. *Lecture notes in computer science volume*, 2018, 11045(5): 13-21.
- [21] JOCHER G, STOKEN A, BOROVEC J, et al. YOLOv5: version 5.0[EB/OL]. (2021-04-12) [2022-05-20]. <https://github.com/ultralytics/yolov5>.
- [22] RONNEBERGER O, FISCHER P, BROX T. U-net: convolutional networks for biomedical image segmentation[C]//Medical Image Computing and Computer-Assisted Intervention-MICCAI 2015: 18th International Conference, October 5-9, 2015, Munich, Germany. Heidelberg: Springer International Publishing, 2015: 234-241.
- [23] LIN T Y, DOLLAR P, GIRSHICK R, et al. Feature pyramid networks for object detection[C]//Proceedings of the IEEE Conference on Computer Vision and Pattern Recognition, July 21-26, 2017, Honolulu, HI, USA. New York: IEEE, 2017: 2117-2125.
- [24] REN S, HE K, GIRSHICK R, et al. Faster R-CNN: towards real-time object detection with region proposal networks[J]. *IEEE transactions on pattern analysis and machine intelligence*, 2015, 39(6): 1137-1149.
- [25] GIRSHICK R. Fast R-CNN[C]//Proceedings of the IEEE International Conference on Computer Vision, December 13-16, 2015, Santiago, Chile. New York: IEEE, 2015: 1440-1448.